Seton Hall University Dissertations and Theses (ETDs)

Winter 12-13-2013

Fumarate Inhibits TNF-α Release

Megan Kelly
megan.kelly2@student.shu.edu

Fumarate Inhibits TNF-α Release
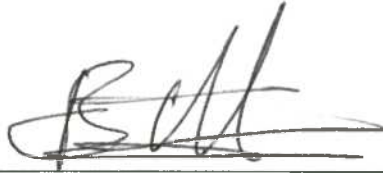

By

Megan L. Kelly

Submitted in partial fulfillment of the requirements for the
degree of Master of Science in Microbiology from the
Department of Biology of Seton Hall University
December 2013

Approved By:

_____
MENTOR
Dr. Allan Blake
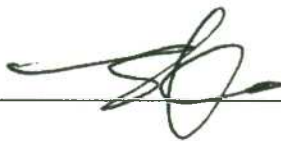
_____
COMMITTEE MEMBER
Dr. Constantine Bitsaktsis

_____
COMMITTEE MEMBER
Dr. Daniel B. Nichols

_____
DIRECTOR OF GRADUATE STUDIES
Dr. Allan Blake

_____
CHAIR PERSON, BIOLOGY DEPARTMENT
Dr. Jane Ko

Acknowledgements

I would like to extend my gratitude to the following people:

Table of Contents

List of Figures

Abstract

Vertebrates utilize two forms of immunity to combat pathogens. Innate immunity is considered the first line of defense that utilizes immediate action and three barriers. Innate immunity responses typically occur within minutes of pathogen exposure resulting in cellular receptor activation and acute pro-inflammatory cytokine release. Inflammatory macrophages engage bacterial endotoxins, including Gram-negative lipopolysaccharide (LPS) and Gram-positive lipoteichoic acid (LTA). And respond by releasing tumor necrosis factor-α (TNF-α). While beneficial for neutralizing acute pathogen exposure, prolonged TNF-α release results in chronic inflammation and tissue damage. In the present study, we examined two methylated derivatives of a citric acid cycle intermediate, fumarate, as potential mediators of endotoxin-induced TNF-α release. We determined that 10μM dimethyl fumarate (DMF) significantly inhibited LPS-mediated soluble TNF-α released from the mouse monocyte cell line RAW 264.7, with no effect on cell viability or reactive oxygen species (ROS) generation. Monomethyl fumarate (MMF) and DMF showed minimal effects on cell viability or ROS generation. We found that DMF at 10μM is anti-inflammatory with minimal monocyte cytotoxicity. The cellular mechanism of DMF action remains unknown.

Introduction

Vertebrates utilize two forms of immunity: innate and adaptive. Innate immunity is considered the first line of defense that utilizes immediate action and three barriers. Physical barriers include the skin and mucous membrane, chemical barriers include stomach acid and antimicrobial properties of specialized soluble molecules, and cellular barriers include cellular receptors that detect microbial products (Kindt, 2007). Innate immunity responses typically occur within minutes of pathogen invasion. And generally, a pathogen evading the innate immune response triggers the adaptive immune response (Kindt, 2007). Adaptive immunity arises from immune B and T cells that detect and respond to a pathogen. Adaptive immunity is the basis for immunological memory, whereby pathogen exposure triggers a cell-mediated immune response that can escalate upon future exposures (Kindt, 2007). Pathogen recognition stimulates T cell diversification and B cell antibody production to orchestrate the immunological defense.

Inflammation is an evolutionary conserved multicellular organismal response (Akira *et al.*, 2006). An acute inflammatory response is initiated during the early stages of infection that involves leukocytes, such as neutrophils and monocytes, which mobilize to contain the triggering event (Kindt, 2007). Vasodilation and vascular permeability increases are hallmarks of the inflammatory response, which allow leukocytes to undergo diapedesis, phagocytize invading pathogens, and synthesize and release soluble chemical mediators identified as chemokines and cytokines (such as tumor necrosis factor-α, TNF-α). A chronic inflammatory response arises when residential immune cells engage in prolonged pro-inflammatory cytokine secretion resulting in altered cellular phenotypes and host tissue remodeling (Kindt, 2007; Hoebe *et al.*, 2004).

1

Immune responses utilize energy and intermediates from metabolic pathways, which include glycolysis, citric acid cycle, electron transport and oxidative phosphorylation. Glycolysis occurs in the cytosol and converts glucose to pyruvate (Berg *et al.*, 2007; Garrett *et al.*, 2010). Pyruvate is transported into the mitochondria where it is converted to acetyl-CoA and oxidized to CO_2 in the citric acid cycle. Oxidation liberates electrons that are delivered by NADH and $FADH_2$ to the structured chain of proteins and coenzymes known as the electron transport chain. Trans-membrane transport of electrons creates a proton gradient across the mitochondrial membrane, which drives ATP production through oxidative phosphorylation. ATP is produced in limited quantities via glycolysis and citric acid cycle with oxidative phosphorylation being largely responsible for meeting an aerobic cell's ATP requirements (Berg *et al.*, 2007; Garrett *et al.*, 2010).

The mitochondria plays a critical role in cell survival, mass production of an aerobic cells ATP supply, but also by influencing apoptosis, cell cycle, and metabolism (Naik and Dixit, 2011; Tschopp, 2011). Oxidation of glucose, pyruvate and NADH result in reactive oxygen species (ROS) as a byproduct, though normally the deleterious effects are removed by antioxidants (Naik and Dixit, 2011). However, several chronic inflammatory diseases also are characterized by excessive ROS production (Naik and Dixit, 2011). ROS perform essential roles in immune responses to pathogens, including death through the production of NADPH oxidases during the respiratory burst in activated macrophages and neutrophils (Bulua *et al.*, 2011). TNF-induced mitochondrial ROS have been implicated in cell death through inhibition of MAPK phosphatases (Bulua *et al.*, 2011). ROS activation of the inflammasome has been questioned as a distinct role for ROS in up-regulation of mRNA for inflammatory cytokines such as TNF (Bulua *et al.*,

2

2011). To avoid cellular damage ROS-generating mitochondria are constantly removed by mitophagy, a form of autophagy or cell death (Tschopp, 2011).

The citric acid cycle is considered a catabolic process due to the oxidation of acetate side chains to CO_2 and providing electrons for the electron transport of ATP and production. The citric acid cycle also fuels multiple biosynthetic processes by transamination of oxaloacetate, succinyl-CoA, α-ketoglutarate, and fumarate. A citric acid cycle intermediate, fumaric acid, is derived from fumarate. Downstream, fumarate can be trans-aminated to produce amino acids aspartate, asparagine, threonine, methionine, isoleucine, and lysine (Garrett *et al.*, 2010). Of considerable interest is that the intermediates in the citric acid cycle have been examined and tested for their immunomodulator capabilities, which could heighten or inhibit particular immune responses (Moharregh-Khiabani *et al.*, 2009).

Fumarate has been examined for anti-inflammatory properties (Moharregh-Khiabani *et al.*, 2009; Gold *et al.*, 2012). In 1959 Dr. Schweckendiek, a German biochemist, hypothesized that a fumarate deficiency in the citric acid cycle was the cause of psoriasis (Asadullah et al., 1997; Mrowietz and Asadullah, 2005; Yazdi and Mrowietz, 2008; Moharregh-Khiabani et al. 2009). Over time he developed a mixture of fumaric acid esters that successfully treated patient psoriasis symptoms, although free fumaric acid was associated with negative gastrointestinal effects (Asadullah et al., 1997; Mrowietz and Asadullah, 2005; Yazdi and Mrowietz, 2008; Moharregh-Khiabani et al. 2009). In 1994, a defined mixture of fumaric acid esters was commercialized under the name Fumaderm (Jong et al., 1998; Mrowietz and Asadullah, 2005; Yazdi and Mrowietz, 2008; Moharregh-Khiabani et al. 2009). Recently, the Food and Drug Administration (FDA) approved Tecfidera (clinical trial name BG-12) as a suitable oral treatment for patients suffering from inflammatory conditions, such as relapse-remitting multiple

3

sclerosis (RRMS) and psoriasis. Tecfidera has been shown to possess anti-inflammatory and neuroprotective properties (FDA, 2013). Fumaderm and Tecfidera have a common main component known as dimethyl fumarate that has been shown to be cell penetrant and hydrolyzed by intracellular esterases to its active metabolite monomethyl fumarate (MMF) (Moharregh-Khiabani et al. 2009).

RAW 264.7 cells, mouse monocyte cell line, has been utilized in prior studies for consistently demonstrating their ability to synthesize and release a host of markers of inflammation and have proven to be a valuable research tool for studying pathological and physiological inflammation in disease (Tweedie *et al.*, 2009). A clustering of ligand interactions based on cytokine production originates from the existence of a limited set of interaction agents that provide the ability to integrate specific signaling pathways to yield unique output responses (Natarajan *et al.*, 2006). RAW 264.7 cells have been shown to have a heterologous stably transfected TNF-α-CAT fusion gene, which can be strongly induced by LPS at the transcriptional level. LPS has been suggested to function through the Raf/Ras signaling pathways that ultimately targets sequence elements present in the 3'-untranslated region (UTR) of TNF-α mRNA (Raabe *et al.*, 1998). RAW 264.7 cells secretes large amounts of TNF-α when LPS-induced and has been extensively characterized. TNF-α mRNA can be detected in unstimulated RAW 264.7 cells then be strongly induced upon LPS-stimulation (Raabe *et al.*, 1998). In the absence of LPS stimulation, RAW 264.7 cells produce small quantifiable amounts of TNF-α mRNA and protein. The increase of TNF-α mRNA and protein levels following LPS stimulation results primarily from transcriptional activation of the TNF-α gene (Raabe *et al.*, 1998).

We utilized RAW 264.7 cells to generate a rapid and reproducible model of inflammation to evaluate dimethyl fumarate (DMF) and its active metabolite monomethyl fumarate (MMF)

4

anti-inflammatory action, cell viability and reactive oxygen species production. Dimethyl fumarate (DMF) and its active metabolite monomethyl fumarate (MMF) have been studied extensively for their anti-inflammatory and neuroprotective properties in various cell types (Jong et al., 1998; Mrowietz and Asadullah, 2005; Yazdi and Mrowietz, 2008; Moharregh-Khiabani *et al.* 2009; Gold *et al.*, 2012). Our results indicate 10μM DMF suppresses endotoxin-stimulated soluble TNF-α with no effect on cell viability or ROS generation.

Methods and Materials

Cell Culture

The Abelson murine leukemia virus transformed macrophage TIB-71[TM] (RAW 264.7) was purchased from American Type Culture Collection (ATCC®, Manassas, VA). RAW 264.7 cells were cultured in sterile 100mm petri dishes and 24-well cell culture dishes (VWR International, LLC , Radnor, PA) in Rosewell Park Memorial Institute 1640, RPMI, (containing GlutaMAX[TM], biotin (0.2mg/L), vitamin B12 (0.005mg/L), PABA (1mg/L), high concentrations of vitamins (3mg/L choline chloride, 0.25mg/L D-calcium pantothenate, 1mg/L folic acid, 1mg/L niacinamide, 1mg/L pyridoxine hydrochloride, 0.2mg/L riboflavin, 1mg/L thiamine hydrochloride, and 35mg/L i-inostitol), and glutathione (1mg/L), Invitrogen[TM]/Life Technologies; Carlsbad, CA). RPMI media was supplemented with 5% fetal bovine serum (V/V) and 1% penicillin/streptomycin (10,000 units/mL penicillin/10,000 μg/mL streptomycin). The cells were incubated at 37°C in a humidified atmosphere of 5% CO_2, 95% air. The cell cultures were passaged at 70% confluence, and plated for experiments 48 to 72 hours.

Fumarate Treatment

RAW 264.7 cells were cultured in 24-well plates with RPMI for 24 hours at 37°C in a humidified atmosphere of 5% CO_2, 95% air. And then treated with either monomethyl fumarate (MMF) or dimethyl fumarate (DMF) (Aldrich, St. Louis, MO) at concentrations of 1mM, 3mM, and 5mM. Monomethyl fumarate samples were diluted in 7.4 pH phosphate buffered saline (PBS) (Invitrogen™/Life Technologies, CA). Dimethyl fumarate samples were diluted in dimethyl sulfoxide (DMSO) (Sigma, St/ Louis, MO). Following treatments, the plates were placed on a shaker at 200rpm for 5 minutes at room temperature then incubated for 2 hours or 24 hours at 37°C in a humidified atmosphere of 5% CO_2, 95% air. The supernatant was collected after incubation and stored at -20°C before analysis. TNF-α was quantified using a commercially available Enzyme Linked Immunoabsorbant Assay (Mouse TNF-α ELISA MAX™ Deluxe kit (BioLegend®; San Diego, CA)).

Endotoxin and Fumarate Treatment

RAW 264.7 cells were cultured in 24-well plates with RPMI for 24 hours at 37°C in a humidified atmosphere of 5% CO_2, 95% air. And then treated with or without endotoxin (1μg/mL) and either monomethyl fumarate (MMF) or dimethyl fumarate (DMF) (Aldrich, St. Louis, MO) at concentrations of 10μM and 15μM. Monomethyl fumarate samples were diluted in 7.4 pH phosphate buffered saline (PBS) (Invitrogen™/Life Technologies, CA). Dimethyl fumarate samples were diluted in dimethyl sulfoxide (DMSO) (Sigma, St/ Louis, MO). The endotoxins utilized were Gram-negative lipopolysaccharide (LPS) and Gram-positive lipoteichoic acid (LTA) (Invitrogen™/Life Technologies, CA) at a concentration of 1μg/mL. Following treatments, the plates were placed on a shaker at 200rpm for 5 minutes at room temperature then incubated for 2 hours or 24 hours at 37°C in a humidified atmosphere of 5% CO_2, 95% air. The supernatant was collected after incubation and stored at -20°C before analysis. TNF-α was quantified using a commercially available Enzyme Linked Immunoabsorbant Assay (Mouse TNF-α ELISA MAX™ Deluxe kit (BioLegend®; San Diego, CA)).

TNF-α ELISA

RAW 264.7 cell supernatants were thawed and then assayed for soluble TNF-α by ELISA. All reagents were used at room temperature.

ELISA assays were carried out according to the manufacturer's instructions. Briefly, a NUNC flat-bottomed 96-well plate was prepared the day before performing the ELISA. The 5X Coating Buffer was diluted with deionized water to prepare a 1X Coating Buffer solution. The 1X Coating Buffer was then used to dilute the pre-titrated Capture Antibody in a 1:200 dilution. The diluted Capture Antibody was then placed into each well at a volume of 100μL. The plate was then sealed and incubated overnight at 4°C.

The following day a 1X Assay Diluent was prepared. The plate was washed four times with 300μL of Wash Buffer (PBS+0.05% Tween-20) per well. After the final addition, the plate was sealed, placed on a plate shaker and incubated at room temperature for 1 hour at 200rpm.

Standards were prepared by serially diluting the 500pg/mL concentration according to manufacturer's instructions and assayed in triplicates at each concentration. To establish accurate cytokine levels, the supernatant of cells treated with LPS or LTA were diluted 1:10 for the exposure period of 2 hours, diluted 1:100 for the exposure period of 24 hours with 1X Assay Diluent and then assayed for soluble TNF-α by ELISA. The plate was washed four times and the standards and samples we added. The plate was then sealed, placed on a plate shaker and incubated at room temperature for 2 hours at 200rpm.

The biotinylated detection antibody was used at 1:200 final dilution. After incubation, each well was washed four times and the detection antibody was added. The plate was then sealed, placed on a plate shaker and incubated at room temperature for 1 hour at 200rpm.

After incubation, the plate was washed four times. For signal detection, Avidin-HRP (final dilution of 1:1000) was added and incubated at room temperature for 30 minutes at 200rpm then washed five times. The 3', 3', 5', 5' tetramethylbenzadine substrate (TMB) was added and the plate was covered. To stop the reaction, 100μL of Stop Solution (2N H_2SO_4) was added to the wells and the resulting substrate colorimetric absorbance was determined at 450nm with a Spectra MAX 250 microplate reader (Molecular Devices, Sunnyvale, CA). The resulting data was stored using the SoftMax Pro 3.0 Software (Molecular Devices, Sunnyvale, CA). The results were then analyzed using GraphPad Prism version 5 (GraphPad Software, Inc., La Jolla, CA).

Cell Viability

RAW 264.7 cells were cultured in 24-well plates with RPMI for 24 hours at 37°C as described above. After incubation the cells were treated with either MMF or DMF over the concentration range of 1nm to 100μM. Following treatment, the plates were placed on the shaker for 5 minutes at room temperature then incubated for 2 hours or 24 hours at 37°C in a humidified atmosphere of 5% CO_2, 95% air.

RAW 264.7 cell viability was assessed with the fluorescent viability dye, calcein-AM (Invitrogen[TM]/Life Technologies, CA) as described (Blake, 2004). Briefly, after treatment the cell monolayers were washed with 1mL PBS and then incubated with 1μg/mL calcein-AM in OptiMEM (Invitrogen[TM]/Life Technologies, CA) containing penicillin/streptomycin (10,000 units/mL penicillin/10,000 μg/mL streptomycin) for 20 minutes at 37°C in a humidified atmosphere of 5% CO_2, 95% air. The monolayers were then washed once with 1mL PBS and retained cellular fluorescence determined using a fluorescent plate reader (CytoFluor II, Perspective Biosystems, MA) with excitation at 485nm and emission at 530nm. The resulting data were exported and analyzed using GraphPad Prism version 5 (GraphPad Software, Inc., La Jolla, CA).

Reactive Oxygen Species Production

RAW 264.7 cells were cultured in 24-well plates with RPMI for 24 hours at 37°C in a humidified atmosphere of 5% CO_2, 95% air. Reactive oxygen production was stimulated 0.003% hydrogen peroxide (H_2O_2), with or without 1μg/mL LPS, and either MMF or DMF at concentrations of 10μM and 15μM. Following treatments, the plates were placed on a rotary shaker for 5 minutes then incubated for 2 hours at 37°C in a humidified atmosphere of 5% CO_2, 95% air.

RAW 264.7 cell reactive oxygen species production was assessed with the fluorescent oxidative stress indicator, 6-chloromethyl 2',7'dichlorodihydrofluorescein diacetate (CM-H2DCFDA; Invitrogen). Briefly, treated plates were washed with 1mL PBS for 1 minute and then incubated with 1μM CM-H2DCFDA in PBS for 20 minutes at 37°C in a humidified atmosphere of 5% CO_2, 95% air. The monolayers were rinsed and the retained cellular fluorescence was quantified with a fluorescent plate reader (CytoFluor II, Perspective Biosystems, MA) with excitation at 485nm and emission at 530nm. The resulting data were exported and analyzed using GraphPad Prism version 5 (GraphPad Software, Inc., La Jolla, CA).

TNF-α release from RAW 264.7 cells

The effects of fumaric acid derivative monomethyl fumarate, MMF, or dimethyl fumarate, DMF, on the murine RAW 264.7 cells were examined at concentrations of 1mM, 3mM and 5mM (Fig. 1). Cells exposed to MMF for 2 hours, resulted in a decrease in released, soluble TNF-α, though the decrease was not statistically significant (Fig. 1A; $P>0.05$). One millimolar MMF, 3mM MMF and 5mM MMF decreased TNF-α by 26% (7.5±1.8pg/mL), 24% (7.7±2.2pg/mL) and 6% (9.5±0.35pg/mL) compared to the untreated control cells (10±1.0pg/mL). as shown in Figure 1B, cells exposed to MMF for a longer period of 24 hours resulted in either a decrease or increase in soluble TNF-α that were not statistically significant when compared to control ($P> 0.05$). Three millimolar MMF resulted in a decrease in soluble TNF-α released by 23% (42±18pg/mL) compared to the untreated control cells (55±16pg/mL). However, 1mM MMF and 5mM MMF increased soluble TNF-α by 90% (103±30pg/mL) and 138% (130±54pg/mL) compared to the untreated control cells. Taken together, these results indicate no statistically significant effects of MMF on basal, soluble TNF-α.

We next examined the ability of DMF to inhibit soluble TNF-α release. Cells were exposed to DMF for 2 hours and the soluble TNF-α response measured was not determined to be statistically significant when compared to the control cells (Fig. 1C; $P>0.05$). Five millimolar DMF resulted in a decrease in soluble TNF-α by 53% (5.1±4.4pg/mL) compared to the untreated control cells (11±4.8pg/mL). However, 1mM DMF and 3mM DMF increased soluble TNF-α by 127% (25±8.5pg/mL) and 5% (12±6.0pg/mL) compared to the corresponding untreated control cells. As shown in Figure 1D, cells exposed to DMF for 24 hours resulted in a decrease in soluble TNF-α release that was not statistically significant ($P>0.05$). At 24 hours, 1mM DMF,

3mM DMF and 5mM DMF decreased soluble TNF-α by 32% (26±9.3pg/mL), 66% (13±6.9pg/mL) and 77% (8.9±3.7pg/mL) compared to the untreated control cells (38±17pg/mL).

MMF and DMF resulted in both increases and decreases in soluble TNF-α release by RAW 264.7 cells, although the results were not statistically different from control, soluble TNF-α levels. Based on these results, MMF and DMF do not significantly impact basal soluble TNF-α release.

We next examined the effects of MMF and DMF on LPS and LTA endotoxin-stimulated TNF-α release at concentrations of either 10μM or 15μM in combination with the Gram-negative endotoxin LPS (1μg/mL; Fig. 2A and 2B) or the Gram-positive endotoxin LTA (1μg/mL; Fig. 2C and 2D). To establish accurate cytokine levels, the supernatant of cells treated with LPS or LTA were diluted 1:10 for the exposure period of 2 hours, diluted 1:100 for the exposure period of 24 hours and then assayed for soluble TNF-α by ELISA. Cells exposed to LPS for 2 hours significantly stimulated a 13-fold increase in soluble TNF-α (188±37pg/mL; ***P<0.001) compared to the untreated control cells (15±2.5pg/ml). The addition of 10μM MMF or 15 μM MMF to the LPS-stimulated cells reduced the LPS-soluble TNF-α by 32% (127±6.7pg/mL) and 30% (132±2.0pg/mL) compared to the LPS-stimulated cells. However, this reduction in soluble TNF-α was not statistically significant (P>0.05). Cells treated with LPS for 2 hours in the presence of 10μM DMF or 15 μM DMF reduced the LPS-stimulated soluble TNF-α by 69% (59±4.4pg/mL; **P<0.01) and 44% (105±17pg/mL; P>0.05) compared to the LPS-stimulated cells (Fig. 2A). LPS-stimulated cells with the addition of 10μM DMF significantly reduced the soluble TNF-α released compared to LPS-stimulated cells.

As shown in Figure 2B, cells exposed to LPS for the longer period of 24 hours significantly stimulated a 4-fold increase (73%) in soluble TNF-α (226±12pg/mL; ***P<0.001)

14

compared to the untreated control cells (62±11pg/mL) due to the longer exposure time. The addition of 10µM MMF or 15µM MMF to the LPS-stimulated cells reduced the LPS-soluble TNF-α by 7% (210±27pg/mL) and 1% (224±30pg/mL) compared to the LPS-stimulated cells. However, this reduction in soluble TNF-α was not statistically significant (P>0.05). Cells treated with LPS for 24 hours in the presence of 10µM DMF or 15 µM DMF significantly reduced the LPS-stimulated soluble TNF-α by 63% (83±16pg/mL; **P<0.01) and 45% (123±17pg/mL; *P<0.05) compared to the LPS-stimulated cells.

These results (Fig. 2A and 2B) show that, at both exposure periods 10µM DMF significantly reduced soluble TNF-α compared to LPS-stimulated cells and LPS-stimulated cells significantly increased soluble TNF-α compared to untreated control cells. At both exposure periods, DMF was more effective than MMF in reducing the release of LPS-stimulated soluble TNF-α from RAW 264.7 cells. Taken together (Fig. 2A and 2B), our results show that 10µM DMF was the more effective concentration for reducing the LPS-stimulated soluble TNF-α at the 2 and 24 hour exposures. Based on these results, it can be concluded that 10µM DMF can be a potential therapy for inappropriate TNF-α release. This can be attributed to the chemical structural difference of DMF having two methyl groups allowing it to cross the cell membrane and to be cleaved by internal esterases into the active metabolite monomethyl fumarate.

We next examined the effects of the Gram-positive bacterial endotoxin, LTA, on soluble TNF-α release from RAW 264.7 cells (Fig. 2C and 2D). Cells exposed to LTA for two hours significantly stimulated a 2.5-fold (144%) increase in soluble TNF-α (35±3.8pg/mL; *P<0.05) compared to the untreated control cells (14±3.8pg/mL). The addition of 10µM MMF or 15µM MMF increased LTA-soluble TNF-α by 8% (38±4.1pg/mL) and 8% (38±1.9pg/mL) compared to the LTA-stimulated cells (P>0.05). Cells treated with LTA for 2 hours in the presence of 10µM

15

DMF reduced the LTA-stimulated soluble TNF-α by 60% (14±1.7pg/mL; **P<0.01) compared to the LTA-stimulated cells. The presence of 10μM DMF in combination with LTA reduced the soluble TNF-α to the basal level of the untreated control cells (14pg/mL). Fifteen micromolar DMF reduced the LTA-stimulated soluble TNF-α by 12% (31±4.8pg/mL; P>0.05) compared to the LTA-stimulated cells (Fig. 2C). LTA-stimulated cells with the addition of 10μM DMF significantly reduced the soluble TNF-α released compared to LPS-stimulated cells. The structural differences between MMF and DMF allow DMF to enter the cell and break down to the active metabolite MMF. MMF does not enter the cell to the extent that DMF does.

As shown in Figure 2B, cells exposed to LPS for the longer period of 24 hours significantly reduced soluble TNF-α by 57% (28±6.7pg/mL; ***P<0.001) compared to the untreated control cells (65±6.0pg/mL). However, if you take into account the dilution of the LTA supernatant the soluble TNF-α increased by 43-fold (2800±670pg/mL) compared to the untreated control. The addition of 10μM MMF to LTA-stimulated cells increased soluble TNF-α by 24% (3500±240pg/mL; P<0.05) compared to the LTA-stimulated cells (2800±670pg/mL). However, the addition of 15μM MMF to LTA-stimulated cells reduced soluble TNF-α by 7% (2600±120pg/mL; P<0.05) compared to the LTA-stimulated cells. Cells treated with LTA for 24 hours in the presence of 10μM DMF or 15μM DMF increased soluble TNF-α by 15% (3200±430pg/mL; P<0.05) and 33% (3700±470pg/mL; P<0.05).

Figure 2C and 2D show that 10μM DMF significantly reduced LTA-stimulated soluble TNF-α at an exposure period of 2 hours compared to the control, LTA-stimulated cells. LTA-stimulated cells significantly increased soluble TNF-α compared to the untreated control cells at both exposure periods. Taken together (Fig. 2C and 2D), our results show that 10μM DMF was the most effective concentration reducing LTA-stimulated soluble TNF-α at 2 hours of exposure.

16

Based on these results, it can be concluded that MMF at both exposure periods and DMF at 24 hours of exposure were not effective in reducing LTA-stimulated soluble TNF-α.
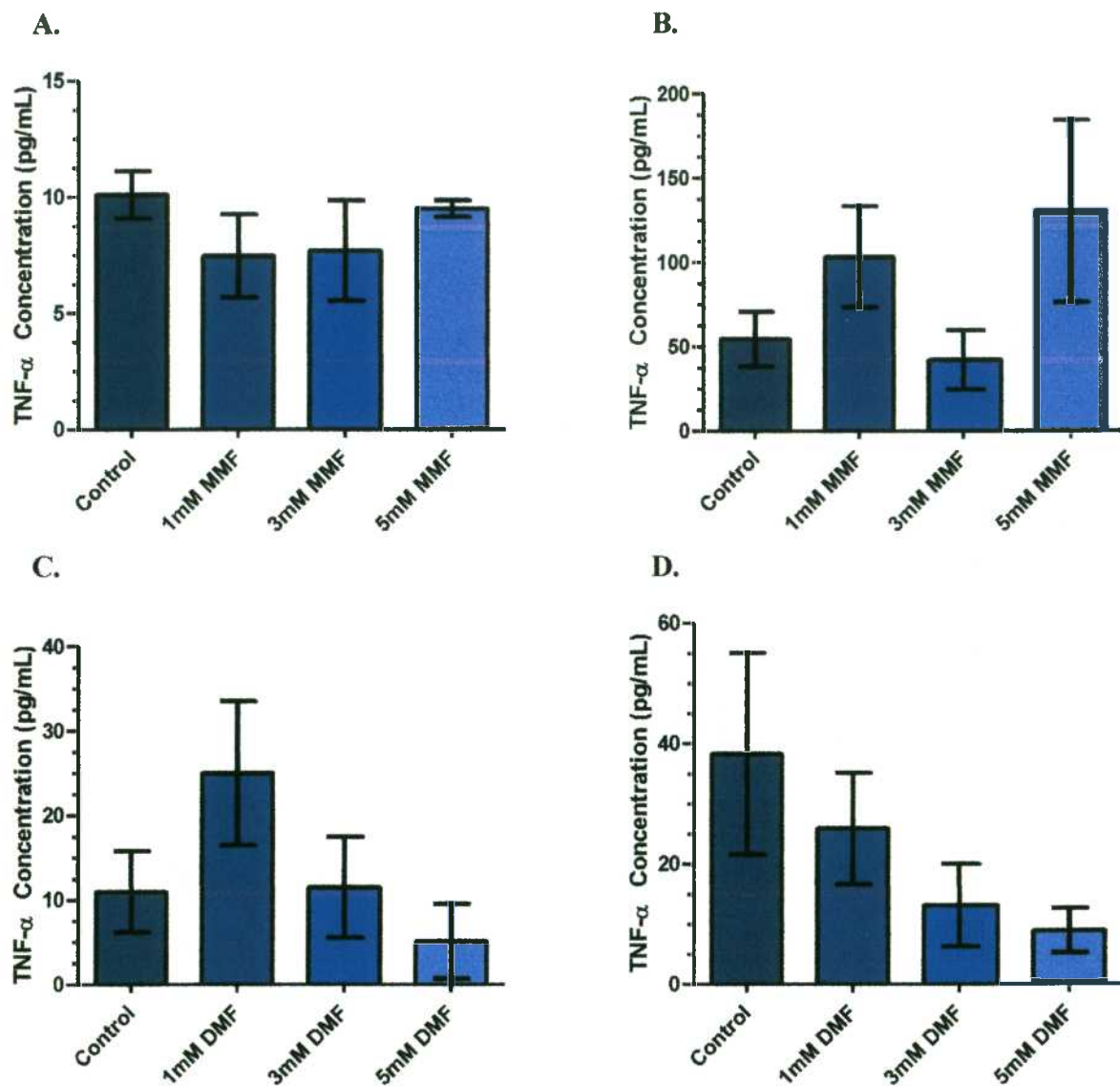
Figure 1. TNF-α release in response to MMF or DMF. RAW 264.7 cells were incubated with 1mM MMF, 3mM MMF, 5mM MMF, 1mM DMF, 3mM DMF, or 5mM DMF. **A and C.** After 2 hours the supernatant was collected to access the concentration of soluble TNF-α released. The results shown are means ± SEM for three 24-well plates, each assayed in triplicate. **B and D.** After 24 hours the supernatant was collected to access the concentration of soluble TNF-α released by ELISA. The results shown are means ± SEM for three 24-well plates, each assayed in triplicate (P> 0.05).
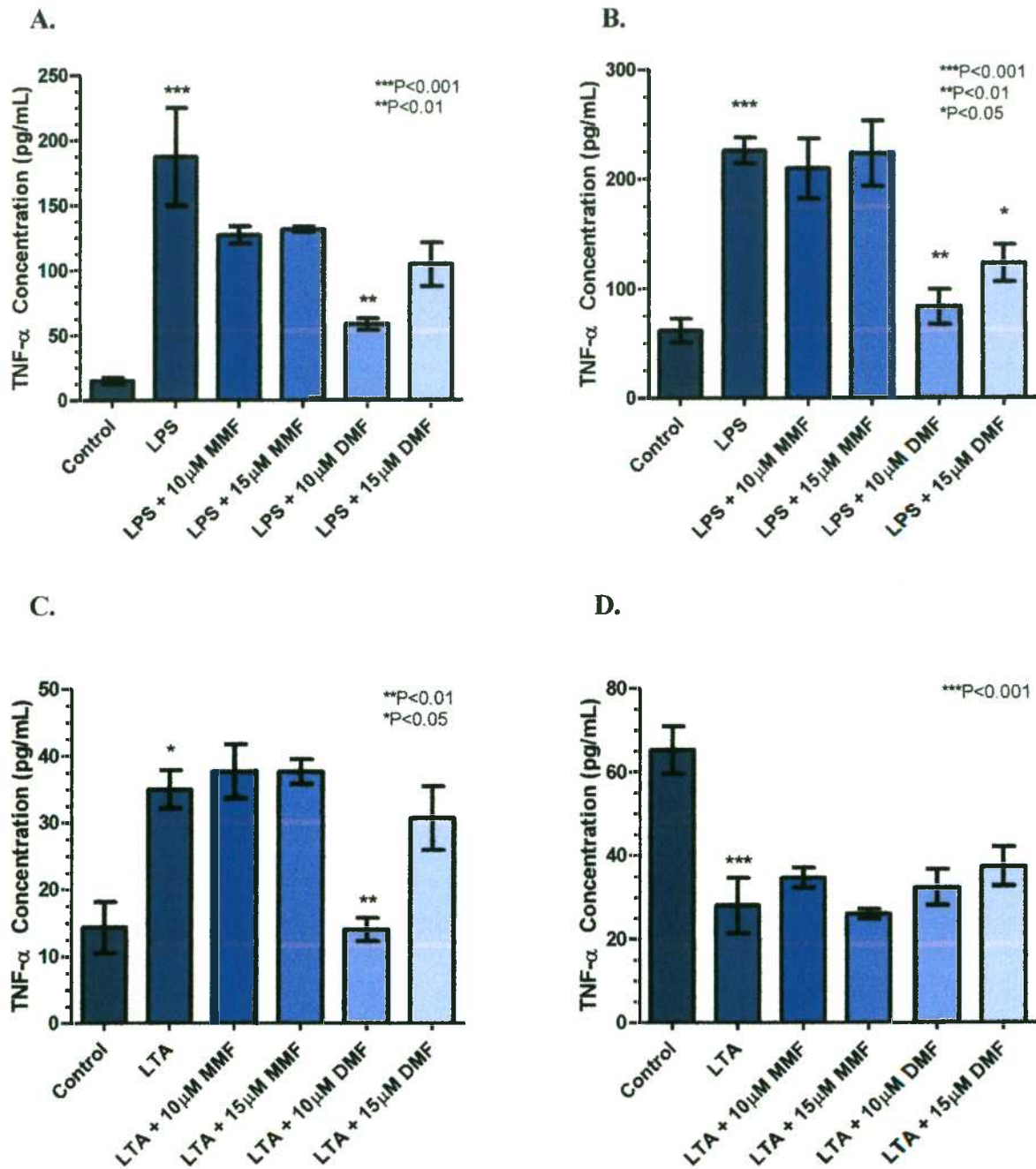
Figure 2. TNF-α release after endotoxin exposure and either MMF treatment or DMF treatment. RAW 264.7 cells were incubated with 10μM MMF, 15μM MMF, 10μM DMF or 15μM DMF, in the presence of 1μg/mL LPS or LTA. **A and C.** After 2 hours the supernatant was collected to access the concentration of soluble TNF-α released. The results shown are means ± SEM for three 24-well plates, each assayed in triplicate. **B and D.** After 24 hours the supernatant was collected to access the concentration of soluble TNF-α released by ELISA. The results shown are means ± SEM for two 24-well plates, each assayed in triplicate. Statistical comparisons via GraphPad PRISM show significance: **A.** ***P< 0.001 Control vs. LPS; **P<0.01 LPS vs. LPS + 10μM DMF. **B.** ***P< 0.001 Control vs. LPS; **P<0.01 LPS vs. LPS + 10μM DMF; and *P<0.05 LPS vs. LPS + 15μM DMF. **C.** *P<0.05 Control vs. LTA; **P<0.01 LTA vs. LTS + 10μM DMF **D.** ***P<0.001 Control vs. LTA.

RAW 264.7 cell viability with MMF and DMF

We next examined the effects of MMF and DMF on cell viability. Mrowietz and Asadullah (2006) showed that DMF induced apoptosis in immune cells, so we generated a concentration response curve, with final MMF and DMF concentrations ranging from 1nM to 100μM (Fig. 3, 4, 5 and 6). A two hour exposure with MMF of increasing concentrations from 1nM to 750nM resulted in an insignificant increase in cell viability when compared to the untreated control cells (7,060±529 F.U.; Fig. 3A). MMF at 250nM increased viability by 30% (9,172±1243 F.U.) compared to the untreated control cells. One nanomolar MMF, 25nM MMF, 75nM MMF and 500nM MMF increased viability 24% (8,776±511 F.U.), 26% (8,907±912 F.U.), 23% (8,713±1027 F.U.) and 25% (8,819±694 F.U.), respectively. The lowest increases in viability were observed at 150nM MMF and 750nM MMF at 11% (7,831±1039 F.U.) and 7% (7,569±796 F.U.) compared to the untreated control cells. However, the increases in viability indicate no statistically significant effects of nanomolar MMF on basal cell viability (P>0.05).

A two hour exposure with MMF (1μM to 100μM) had a variable response on cell viability, though not a statistically significant effect. MMF at 1μM, 10μM and 15μM reduced viability by 3% (9,295±501 F.U.), 7% (8,867±803 F.U.) and 7% (8,916±346 F.U.), respectively, compared to the untreated control cells (9,538±569 F.U.). However, 50μM MMF, 75μM MMF and 100μM MMF increased viability by % (10,323±522 F.U.), 8% (10,318±615 F.U.) and 3% (9,864±836 F.U.), respectively, compared to the untreated control cells. In contrast, 25nM MMF decreased viability by 0.3% compared to the untreated control cells (Fig. 3B; P>0.05).

A two hour concentration response curve for DMF demonstrated a variable cell viability response, although no statistically significant effect was observed. A reduction in viability was observed at 25nM DMF, 75nM DMF and 150nM DMF by 20% (4,220±437 F.U.), 28%

20

(3,799±353 F.U.) and 38% (3,272±262 F.U.), respectively, compared to the untreated control cells (5,272±529 F.U.; P>0.05; Fig. 4A). DMF at 1nM, 250nM and 750nM reduced viability by 4% (5,070±825 F.U.), 12% (4,628±470 F.U.) and 14% (4,545±396 F.U.), respectively, compared to the untreated control cells (P>0.05). However, DMF at 500nM increased viability by 3% (5,416±1035 F.U.) compared to the untreated control cells (P>0.05).

As seen in Figure 4B, a two hour exposure period with DMF (1μM to 100μM) resulted in a reduction in cell viability throughout the concentration response curve though the decrease was not statistically significant. Ten micromolar DMF and 50μM DMF reduced viability by 9% (6,081±285 F.U.) and 7% (6,222±723 F.U.) compared to the untreated control cells (6,671±517 F.U.; P>0.05). MMF at 15μM, 25μM and 75μM reduced viability by 13% (5,826±348 F.U.), 13% (5,807±308 F.U.) and 19% (5,423±547 F.U.), respectively, compared to the untreated control cells (P>0.05). The highest reduction in viability was observed at 1μM and 100μM reducing viability 26% (4,946±578 F.U.) and 23% (5,155±474 F.U.) compared to the untreated control cells (P>0.05).

We next examined the effects of MMF and DMF on cell viability with an exposure period of 24 hours. A twenty-four hour exposure with MMF (1nM to 750nM) resulted in a variable response in cell viability, although not statistically significant (Fig. 5A). Twenty-five nanomolar MMF, 150nM MMF and 500nM MMF increased viability by 3% (13,801±355 F.U.), 7% (14,400±777 F.U.) and 5% (14,090±1101 F.U.), respectively, compared to the untreated control cells (13,460±935 F.U.; P>0.05). MMF at 75nM, 250nM and 750nM increased viability by 12% (15,041±935 F.U.), 13% (15,212±765 F.U.) and 11% (14,987±805 F.U.), respectively, compared to the untreated control cells (P>0.05). However, a reduction in viability was observed

21

at 1nM MMF by 19% (10,898±759 F.U.) compared to the untreated control cells which was not statistically significant (P>0.05).

As shown in Figure 5B, a 24 hour exposure to MMF (1μM to 100μM) resulted in insignificant reductions in cell viability. Ten micromolar MMF, 25μM MMF and 50μM MMF reduced viability by 6% (18,282±779 F.U.), 8% (17,785±817 F.U.) and 6% (18,182±757 F.U.), respectively, compared to the untreated control cells (19,358±2244 F.U.; P>0.05). MMF at 1μM, 15μM and 100μM reduced viability by 16% (16,263±972 F.U.), 19% (15,725±787 F.U.) and 11% (17,281±539 F.U.), respectively, compared to the untreated control cells (P>0.05). In contrast, 75μM MMF increased viability by 0.3% compared to the untreated control cells (P>0.05).

Although Figures 3, 4 and 5 suggest increases and decreases in cell viability with respect to MMF and DMF at 2 hours of exposure and MMF at 24 hours of exposure, the concentration response curves show no significant increase or decrease in cell viability. The insignificant increases and decreases show that at the exposures times for MMF and DMF the concentrations are not toxic to the cell due to fumarate being an intermediate of the citric acid cycle. The fumaric acid derivatives can be utilized in the cells citric acid cycle and the CO_2 oxidized can enter the electron transport chain. However, once the CO_2 can lead to toxic or non-toxic effects depending upon the results from the electron transport chain.

Exposure to DMF (1nM to 750nM) for 24 hours resulted in a reduction in cell viability that was statistically significant (Fig. 6A). One nanomolar DMF, 25nM DMF, 500nM DMF and 750nM DMF reduced viability by 34% (8,303±840 F.U.; *P<0.05), 35% (8,196±1148 F.U.; *P<0.05), 35% (8,210±640 F.U.; *P<0.05) and 35% (8,135±823 F.U.; *P<0.05), respectively, compared to the untreated control cells (12,614±472 F.U.). The highest reduction in cell viability

22

was observed in the response curve at 150nM and 250nM by 43% (7,166±584 F.U.; **P<0.01) and 40% (7,594±658 F.U.; **P<0.01) compared to the untreated control cells. However, 75 nM DMF reduced viability by 15% (10,664±1406 F.U.; P>0.05) compared to the untreated control cells.

As seen in Figure 6B, DMF (1μM to 100μM) resulted in an insignificant increase and decrease in cell viability (P>0.05). Fifty micromolar DMF and 75μM DMF reduced viability by 7% (11,726±940 F.U.) and 5% (12,039±1299 F.U.) compared to the untreated control cells (12,652±2407 F.U.). DMF at 1μM, 10μM and 100μM reduced viability by 16% (10,650±1223 F.U.), 19% (10,244±832 F.U.) and 26% (9,405±1078 F.U.) compared to the untreated control cells. In contrast, 15μM DMF and 25μM DMF increased viability by 6% (13,372±1322 F.U.) and 4% (13,181±900 F.U.) compared to the untreated control cells.

These results (Fig. 6A and 6B) show that DMF acts in an opposite manner at 24 hours of exposure than at an exposure period of 2 hours. DMF in the concentration response curve range (1nM to 750nM) resulted in statistically significant reduction in cell viability at 1nM, 25nM, 150nM, 250nM, 500nM and 750nM compared to the untreated control cells. Based on the results, exposure to nanomolar DMF is detrimental to the viability of RAW 264.7 cells.

A.

B.
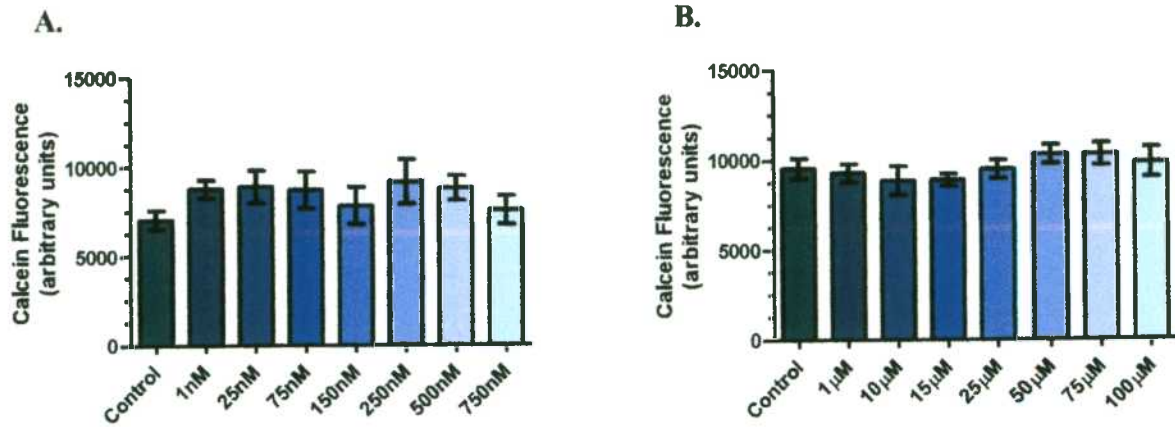
Figure 3. A MMF concentration response curve (1nM to 100µM). RAW 264.7 cell monolayers were incubated for 2 hours in the presence or absence of MMF **A.** After treatment with MMF (1nM to 750nM), cell viability was determined with calcein-AM fluorescence. **B.** After treatment with MMF (1µM to 100µM), cell viability was determined with calcein-AM fluorescence. The results presented are means ± SEM for three 24-well plates, each assayed in triplicate ($P>0.05$).

A.

B.
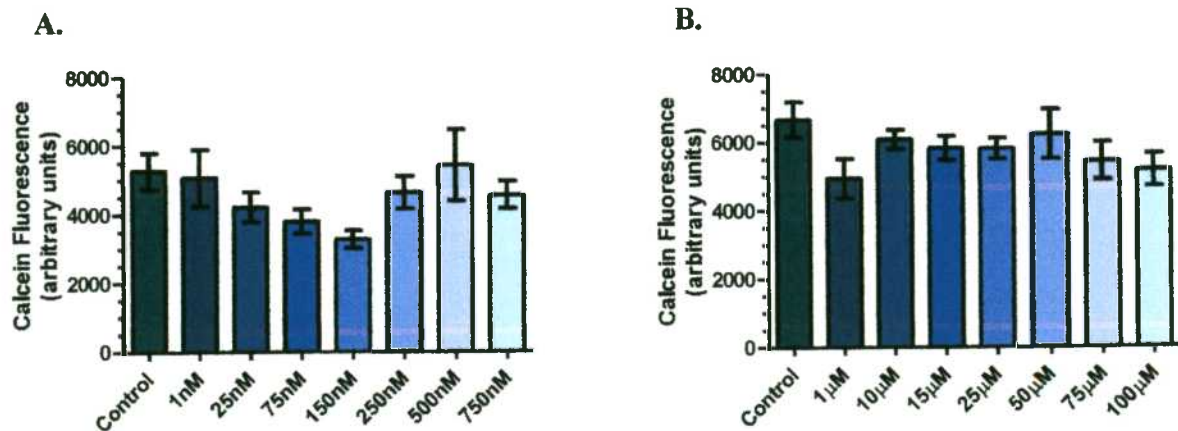
Figure 4. A DMF concentration response curve (1nM to 100µM). RAW 264.7 cell monolayers were incubated for 2 hours in the presence or absence of DMF **A.** After treatment with DMF (1nM to 750nM), cell viability was determined with calcein-AM fluorescence. **B.** After treatment with DMF (1µM to 100µM), cell viability was determined with calcein-AM fluorescence. The results presented are means ± SEM for three 24-well plates, each assayed in triplicate ($P>0.05$).

24
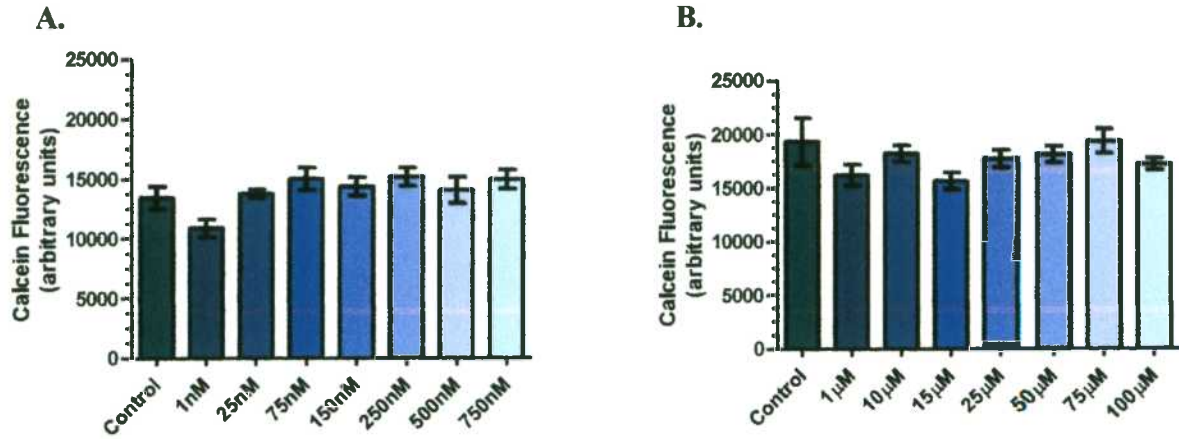
Figure 5. A MMF concentration response curve (1nM to 100µM). RAW 264.7 cell monolayers were incubated for 24 hours in the presence or absence of MMF **A.** After treatment with MMF (1nM to 750nM), cell viability was determined with calcein-AM fluorescence. **B.** After treatment with MMF (1µM to 100µM), cell viability was determined with calcein-AM fluorescence. The results presented are means ± SEM for three 24-well plates, each assayed in triplicate (P>0.05).

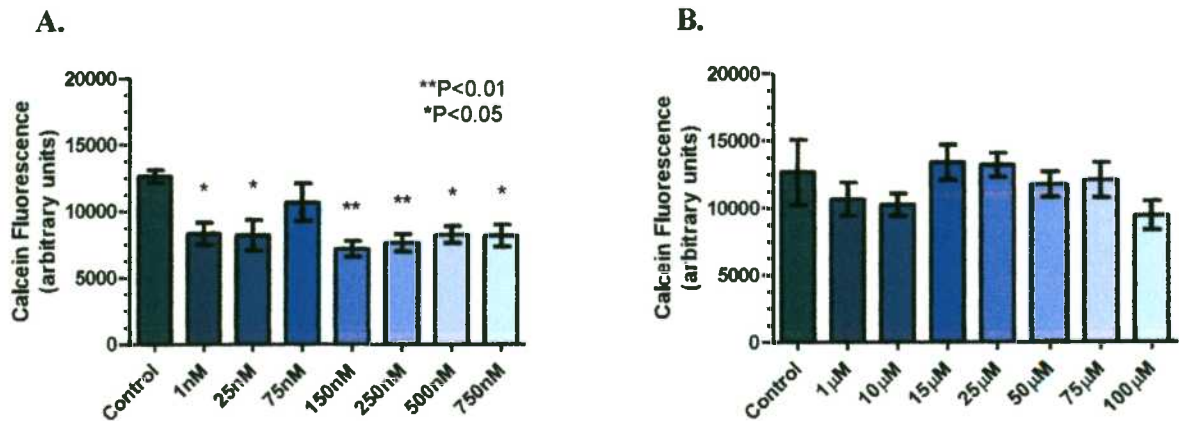

Figure 6. A DMF concentration response curve (1nM to 100µM). RAW 264.7 cell monolayers were incubated for 24 hours in the presence or absence of DMF. **A.** After treatment with DMF (1nM to 750nM), cell viability was determined with calcein-AM fluorescence. **B.** After treatment with DMF (1µM to 100µM), cell viability was determined with calcein-AM fluorescence. Statistical comparisons via GraphPad PRISM show significance: **A.** *P<0.05 Control vs. 1nM DMF, *P<0.05 Control vs. 25nM DMF, **P<0.01 Control vs. 150nM DMF, **P<0.01 Control vs. 250nM DMF, *P<0.05 Control vs. 500nM DMF and *P<0.05 Control vs. 750nM DMF. **B.** P>0.05

25

Reactive Oxygen Species Production with MMF and DMF

We next examined the effects MMF and DMF had on the production of reactive oxygen species (ROS). Albrecht et al. (2012) showed that DMF at low concentrations protected neuronal cells from oxidative stress. Gold et al. (2012) showed fumaric acid esters have the potential to induce the Nrf-2 pathways thereby increasing the pathways ability to mediate neuroprotective effects. So we used MMF and DMF at concentrations of $10\mu M$ and $15\mu M$ alone and in combination with hydrogen peroxide (H_2O_2; 0.003%) and Gram-negative endotoxin LPS ($1\mu g/mL$) for an exposure period of two hours (Fig. 7).

We first stimulated RAW 264.7 with LPS and the addition of $10\mu M$ MMF, $15\mu M$ MMF, $10\mu M$ DMF or $15\mu M$ DMF, which results in an insignificant variation in ROS production compared to the untreated control cells (646 ± 3.0 F.U.; $P>0.05$). Due to the insignificant reduction in ROS production, we added a known ROS, hydrogen peroxide (3%), to the cells to produce ROS.

To examine if ROS were produced by cells, the cells were stimulated with hydrogen peroxide as a means of a positive control that resulted in an insignificant increase ($P>0.05$). We exposed cells to H_2O_2 and combinations of H_2O_2 with MMF or DMF. Cells were exposed to H_2O_2, H_2O_2 with LPS and $10\mu M$ MMF, H_2O_2 with LPS and $15\mu M$ MMF, H_2O_2 with LPS and $10\mu M$ DMF and H_2O_2 with LPS and $15\mu M$ DMF that resulted in an insignificant variation in ROS production compared to the untreated control cells. The addition of the hydrogen peroxide resulted in insignificant ROS production. To see if MMF and DMF themselves had an effect on ROS production, we treated with MMF and DMF alone to account for their effects.

To examine the effect that MMF and DMF have alone on ROS production, we exposed cells to 10µM MMF, 15µM MMF, 10µM DMF and 15µM DMF that resulted in a marginal though insignificant increase in ROS production (P>0.05).

These data (Fig. 7) suggest that MMF and DMF alone or in combination with LPS and H_2O_2 did not significantly increase or decrease ROS production. Future experimentation will be required to determine if MMF and DMF can inhibit ROS production.
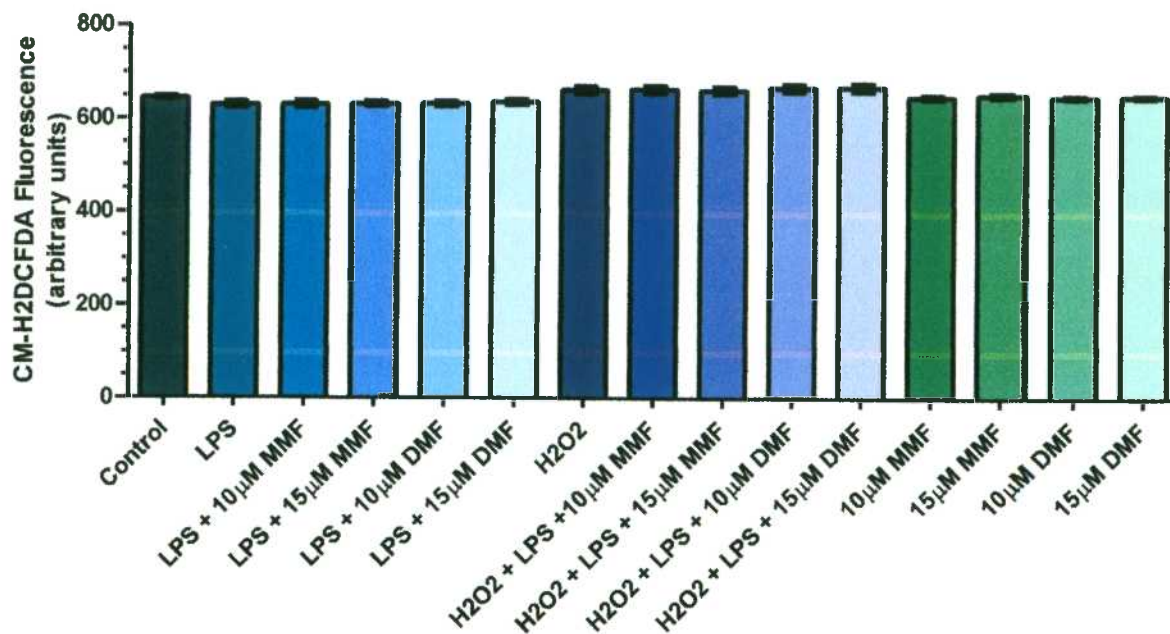
Figure 7. Reactive oxygen species (ROS) production with MMF and DMF with hydrogen peroxide (H_2O_2) and LPS (1μg/mL). RAW 264.7 cells were incubated with 10μM MMF, 15μM MMF, 10μM DMF or 15μM DMF, in the presence or absence of 0.003% H_2O_2 and 1μg/mL LPS for 2 hours. ROS production was determined by CM-H2DCFDA fluorescence and the results presented are means ± SEM for three 24-well plates, each assayed in quadruple (P>0.05).

Discussion

The host's defense mechanisms are important on its survivability. Classically activated macrophages are products of the cell-mediated immune response signals, interferon-γ (IFNγ) and tumor-necrosis factor (TNF). Classically activated macrophages are vital to the host defense, although their actions are tightly regulated due to tissue damage cytokines and mediators can produce (Mosser and Edwards, 2008). If this process becomes deregulated it can lead to several autoimmune diseases, including rheumatoid arthritis, inflammatory bowel disease and multiple sclerosis. The detrimental effects of deregulated cytokine release and ways to inhibit their release have become increasingly researched. Dimethyl fumarate has been utilized since 1959 to treat psoriasis in Germany and in 2013 to treat relapse-remitting multiple sclerosis (FDA, 2013).

The differences in immune response also correlate to damage that may occur. We utilized exposure periods of 2 and 24 hours to emulate acute and chronic inflammation as describe in previous literature were fumarate was utilized as treatment. Furthermore, previous literature showed serum peak concentration of 20μM for the active metabolite MMF, therefore we utilized concentrations at 10μM and 15μM to determine the effects MMF and DMF had on TNF-α secretion, cell viability, and ROS production (Gold *et al.*, 2012). Although the titration range for treatment could be far larger, the range was limited due to previous literature stating DMF induced apoptosis in immune cells at high concentration up to 100μM (Mrowietz and Asadullah, 2006).

LPS has been shown to trigger the wide spread production of TNF-α by macrophages (Feghali and Wright, 1997). Treatment of macrophages or adherent mononuclear cells with LTA has been shown to induce TNF-α (Grunfeld *et al.*, 1999). In the present study, we showed an increase in soluble TNF-α with cells stimulated with LPS or LTA compared to basal levels

29

(Figure 2). Previous literature states 10μM DMF attenuated TNF-α production (Albrecht *et al.*, 2012), which was seen in cells stimulated with LPS and LTA (Fig. 2A, 2B and 2C). DMF has been shown to alter the cytokine levels in cell culture (Ockenfels *et al.*, 1998). We have shown that 15μM has also reduced TNF-α from cells stimulated with LPS or LTA (Fig. 2A, 2B and 2C).

The active metabolite, monomethyl fumarate, used in peripheral blood mononuclear cells (PBMC) and monocytes induced TNF-α in the presence or absence of LPS-stimulated cells for 2 and 24 hours (Asadullah *et al.*, 1997). MMF addition to LPS-stimulated or LTA-stimulated cells reduced and increased soluble TNF-α, although MMF did not reduce to the same level as DMF (Figure 2). This could be due to DMF being more lipophilic than MMF, which allows DMF to enter the cell at a faster rate and in larger quantities compared to MMF (Yazdi and Mrowietz, 2008).

Previous literature showed that DMF induced apoptosis in monocyte derived dendritic cells and T cells (Mrowietz and Asadullah, 2006). The concentration response curve showed significant reduction in cell viability in the nanomolar range of DMF for 24 hours of exposure (Figure 6). Out results are not consistent with those observed by Albrecht *et al.* (2012) where 100μM DMF caused an increase in cell death by apoptosis. Moharregh-Khiabani *et al.* (2009) and Gold *et al.* (2012) observed DMF at higher concentrations induced apoptosis in all cell types. A potential explanation for our results differing can be the incubation time or the cell normal microenvironment. Further experimentation would have to occur to determine if the results we obtain do not correlate with the literature.

The survival of the cell is dependent upon the adaptability of responding to outside stimulus and applying mechanisms to combat the stimulus. Previous literature showed DMF has

30

potential for protecting cells from oxidative stress (Albrecht *et al.*, 2012 and Gold *et al.*, 2012). Activated macrophages and neutrophils utilize ROS to perform essential roles in immune responses to pathogens, which include death through the production of NADPH oxidases during the respiratory burst (Bulua *et al.*, 2011). The deleterious effects which normally occur if left untreated can be removed by antioxidants. Nrf-2 (nuclear factor (erythroid-derived-2)-like 2) pathway has been implicated as the neuroprotective mechanism utilized by DMF and MMF (Scannevin *et al.*, 2012; Linker *et al.*, 2011; Wilms *et al.*, 2010). LPS, tumor-necrosis factor (TNF), and reactive oxygen species/reactive nitrogen sepecies all activate autophagy, and it is well known that LPS triggers ROS production (Yuan *et al.*, 2009). FAE induced an upregulation of the production of superoxide anion in monocytes (Moharregh-Khiabani *et al.*, 2009) DMF interferes with the cellular redox system by modulating intracellular thiols and thereby increasing the level of reduced glutathione. DMF decreased the LPS induced production of TNF-α and increased the cellular glutathione (Gold *et al.*, 2011). Our results had insignificant variation comparing the treated cells with the untreated control cells. RAW 264.7 cells become macrophages when placed onto the treated surface of a well plate, which could potentially explain why the treatments did not affect the cells. A more potent positive control, a higher percentage of hydrogen peroxide, peroxyl radical or hydroxyl radical, may provide valuable insight on if MMF and DMF can protect the cells. With a new positive control, we could make a better determination on if MMF and DMF have neuroprotective effects. From this data we could explore the pathway utilized to protect the cell or verify previous literature stating the Nrf-2 pathway.

The reduction of soluble TNF-α from LPS-stimulated or LTA-stimulated cells, cell viability, and reactive oxygen species production could be attributed to autophagy. The cells can

31

undergo autophagy if they are presented with signals or outside stimulus. Autophagy is active at basal levels in most cell types where it is postulated to play a housekeeping role in maintaining the integrity of the cell. However, autophagy is strongly induced by starvation and is a key component of the adaptive response of cells and organisms to undergo nutrient deprivation that promotes survival until nutrients are available again. Autophagy is generally thought of as a survival mechanism, although its deregulation has been linked to non-apoptotic cell death (Glick *et al.*, 2011).

In summary, we have found that $10\mu M$ DMF significantly reduced soluble TNF-α release from murine monocyte cell line RAW 264.7. We found nanomolar DMF significantly reduced cell viability. Reactive oxygen species were not produced or inhibited to a detectable level in all treatments. The significant reduction in soluble TNF-α, cell viability was maintained, and reactive oxygen species were not produced at $10\mu M$ DMF would indicate that this concentration has the potential to treat the detrimental effects of deregulated cytokine release.

Conclusions

In the present study, we examined two methylated derivatives of fumarate, DMF and MMF. We determined that 10µM DMF significantly inhibited soluble TNF-α released from murine monocyte cell line RAW 264.7 cells stimulated with LPS with no effect on cell viability or ROS generation. MMF and DMF had minimal effects on cell viability. Reactive oxygen species generation was unaltered by DMF treatment. The significant reduction in soluble TNF-α, maintained cell viability and lack of reactive oxygen species indicate DMF at 10µM is anti-inflammatory with minimal monocyte cytotoxicity.

Despite, clear clinical utility, the cellular mechanism of DMF action remains unknown. Future studies focusing on monocyte cellular metabolism, pro-inflammatory gene transcription, translation, processing and release might provide valuable insights. For example, DMF may impact the post-translational processing and membrane presentation of TNF-α. By utilizing flow cytometry in conjunction with TNF-α selective antisera the plasma membrane presentation could be monitored. Establishing the intracellular target of DMF might also provide the groundwork for future small molecule anti-inflammatory molecules.

Furthermore, changing the cell line to a neuroblastoma N-type could provide valuable insight to the mechanisms which MMF and DMF have on neuronal cells. The concentrations of fumarate can be titrated in a wider fashion to determine the most suitable concentration for future studies. Various autoimmune disorders affect the nervous system in some manner, therefore finding suitable treatments for these diseases have the potential to find cures in time.

Literature Cited

Akira, S., Uematsu, S., & Takeuchi, O., (2006). Pathogen recognition and innate immunity. *Cell, 124*(783 – 801)

Albrecht, P., Bouchachia, I., Goebels, N., Henke, N., Hofstetter, H., Issberner, A., Kovacs, Z., Lewerenz, J., Lisak, D., Maher, P., Mausberg, A., Quasthoff, K., Zimmermann, C., Hartung, H. & Methner, A. (2012). Effects of dimethyl fumarate on neuroprotection and immunomodulation. *Journal of Neuroinflammation, 9*:163 (1 – 10)

Asadullah, K., Schmid, H., Friedrich, M., Randow, F., Volk, H.D., Sterry, W., & Docke, W.D. (1997) Influence of monomethylfumarate on monocytic cytokine formation – explanation for adverse and therapeutic effects in psoriasis. *Arch Dermatol Res, 289*(623 – 630)

Berg, J. M., Tymoczko, J. L., & Stryer, L. (2007). *Biochemistry.* (6th ed.). New York, NY: W.H. Freman and Company.

Bhattacharyya, S., Dudeja, P.K., & Tobacman, J.K. (2008). Lipopolysaccharide activates NF-κB by TLR4-Bcl10-dependent and independent pathways in colonic epithelial cells. *Am J Physiol Gastrointest Liver Physiol* 295(G784 – G790)

Blake, A.D. (2004). Dipyridamole is neuroprotective for cultured rat embryonic cortical neurons. *Biochemical and Biophysical Research Communications, 314*(501 – 504)

Bulua, A.C., Simon, A., Maddipati, R., Pelletier, M., Park, H., Kim, K., Sack, M.N., Kastner, D.L. & Siegel, R.M. (2011) Mitochondrial reactive oxygen species promote production of proinflammatory cytokines and are elevated in TNFR1-associated periodic syndrome (TRAPS). *Journal of Experimental Medicine, 208:3*(519 – 533)

Cross, S.A., Cook, D.R., Chi, A.W.S., Vance, P.J., Kolson, L.L., Wong, B.J., Jordan-Sciutto, K.L., & Kolson, D.L. (2011). Dimethyl fumarate, an immune modulator and inducer of antioxidant response, suppresses HIV replication and macrophage-mediated neurotoxicity: a novel candidate for HIV neuroprotection. *The Journal of Immunology, 187*(4049)

Duffy, S., So, A., & Murphy, T.H. (1998). Activation of endogenous antioxidant defenses in neuronal cells prevents free radical-mediated damage. *Journal of Neurochemistry,* 71 (69 – 77)

Feghali, C.A. and Wright, T.M. (1997). Cytokines in acute and chronic inflammation. *Frontiers in Bioscience, 2*(12 – 26)

Fink, M. (2007). Ethyl pyruvate: a novel treatment for sepsis. *Current Drug Targets, 8*(515 – 518)

Garrett, R. H., & Grisham, C. M. (2010). *Biochemistry*. (4th ed.). Boston, MA: Brooks/Cole.

Glick, D., Barth, S., & Macleod, K.F. (2010). Autophagy: cellular and molecular mechanisms. *J Pathol, 221:1*(3 – 12)

Gold, R., Linker, R.A., & Stangel, M. (2012). Fumaric acid and its esters: an emerging treatment for multiple sclerosis with antioxidative mechanism of action. *Clinical Immunology, 142*(44 – 48)

Groesdonk, H.V., Schlottmann, S., Richter, F., Georgieff, M. & Senftleben, U. (2006). *Escherichia coli* prevents phagocytosis-induced death of macrophages via classical NF-κB signaling, a link to T-cell activation. *Infection and Immunity, 74:10*(5989 – 6000)

Grunfeld, C., Marshall, M., Shigenaga, J.K., Moser, A.H., Tobias, P., & Feingold, K.R. (1999). Lipoproteins inhibit macrophage activation by lipoteichoic acid. *Journal of Lipid Metabolism, 40*(245 – 252)

Haddad, J.J. and Land, S.C. (2002). Redox/ROS regulation of lipopolysaccharide-induced mitogen-activated protein kinase (MAPK) activation and MAPK-mediated TNF-α biosynthesis. *British Journal of Pharmacology, 135*(520 – 536)

Hancock, R.E.W., and Scott, M.G. (2000). The role of antimicrobial peptides in animal defenses. *PNAS 97:16*(8856 – 8861)

Heigold, S. and Bauer, G. (2002). RAW 264.7 macrophages induce apoptosis selectively in transformed fibroblasts: intercellular signaling based on reactive oxygen and nitrogen species. *Journal of Leukocyte Biology, 72*(554 – 563)

Hoebe, K., Janssen, E., & Beutler, B. (2004). The interface between innate and adaptive immunity. *Nature Immunology, 5:10,*(971 – 974)

Hoefnagel, J.J., Thio, H.B., Willemze, R., & Bouwes Bavinck, J.N. (2003). Long-term safety aspects of systemic therapy with fumaric acid esters in severe psoriasis. *British Journal of Dermatology, 149*(363 – 369)

de Jong, R., Bezemer, A.C., Zomerdijk, T.P.L., van de Pouw-Kraan, T., ottenhoff, T.H.M., & Nibbering, P.H. (1996). Selective stimulation of T helper 2 cytokine responses by the anti-psoriasis agent monomethylfumarate. *Eur. J. Immunol., 26*(2067 – 2074)

Kindt, T. J., Goldsby, R. A., & Osborne, B. A. (2007). *Kuby immunology*. (6th ed.). New York, NY: W.H. Freeman and Company.

Lehmann, J.C.U., Listopad, J.J., Rentzsch, C.U., Igney, F.H., von Bonin, A., Hennekes, H.H., Asadullah, K., & Docke, W.D.F. (2007). Dimethylfumarate induces immunosuppression via glutathione depletion and subsequent induction of heme oxygenase 1. *Journal of Investigative Dermatology, 127* (835 – 845)

Linker, R.A., Lee, D., Ryan, S., van Dam, A.M., Conrad, R., Bista, P., Zeng, W., Hronowsky, X., Buko, A., Chollate, S., Ellrichmann, G., Bruck, W., Dawson, K., Goelz, S., Wiese, S., Scannevin, R.H., Lukashev, M., & Gold, R. (2011). Fumaric acid esters exert neuroprotective effects in neuroinflammation via activation of the Nrf2 antioxidant pathway. *BRAIN A Journal of Neurobiology 134(678 – 692)*

Litjens, N.H.R., Rademaker, M., Ravensbergen, B., Rea, D., van der Plas, M.J.A., Thio, B., Walding, A., van Dissel, J.T., & Nibbering, P.H. (2004). *Eur. J. Immunol., 34*(565 – 575)

Lowe, R., Pillinger, M., de Martin, R., Mrowietz, U., Groger, M., Holnthoner, W., Wolff, K., Wiegrebe, W., Jirovsky, D., Petzelbauer, P. (2001). Dimethylfumarate inhibits tumor-necrosis-factor-induced CD62E expression in an NF-κB-dependent manner. *J Invest Dermaol, 117*(1363 – 1368)

Meissner, M., Valesky, E.M., Kippenberger, S., & Kaufmann, R. (2012). Dimethyl fumarate – only an anti-psoriatic medication? *Journal of the German Society of Dermatology, 10*(793 – 801)

Miller, L. and Hunt, J.S. (1998). Regulation of TNF-α production in activated mouse macrophages by progesterone. *J. Immunol., 160*(5098 – 5104)

Moharregh-Khiabani, D., Linker, R.A., Gold, R., & Stangel, M. (2009). Fumaric acid and its esters: an emerging treatment for multiple sclerosis. *Current Neuropharmacology, 7*(60 – 64)

Mosser, D.M. (2003). The many faces of macrophage activation. *Journal of Leukocyte Biology, 73*(209 – 212)

Mosser, D.M. and Edwards, J.P. (2008). Exploring the full spectrum of macrophage activation. *Nat Rev Immunol. 8:12*(958 – 969)

Mrowietz, U., and Asadullah, K. (2005). Dimethylfumarate for psoriasis: more than a dietary curiosity. *TRENDS in Molecular Medicine, 11:1*(43 – 48)

Mrowietz, U. Christophers, E. & Altmeyer, P. (1999). Treatment of severe psoriasis with fumaric acid esters: scientific background and guidelines for therapeutic use. *British Journal of Dermatology, 141*(424 – 429)

Naik, E., and Dixit, V.M. (2011). Mitochondrial reactive oxygen species drive proinflammatory cytokine production. *Journal of Experimental Medicine, 208:3*(417 – 420)

Natarajan, M., Lin, K.M., Hsueh, R.C., Sternweis, P.C., & Ranganathan, R. (2006). A global analysis of cross-talk in mammalian cellular signaling network. *Nature Cell Biology, 8:6*(571 – 580)

Nau, G.J., Richmond, J.F.L., Schlesinger, A., Jennings, E.G., Lander, E.S., & Young, R.A. (2002). Human macrophage activation programs induced by bacterial pathogens. *PNAS 99:3*(1503 – 1508)

Nibbering, P.H., Thio, B., Zomerdijk, T.P.L., Bezemer, A.C., Beijersbergen, R.L., van Furth, R. (1993). Effects of monomethylfumarate on human granulocytes. *J Invest Dermatol, 101*(37 – 42)

Ockenfels, H.M., Schultewolter, T., Ockenfels, G., Funk, R., & Goos, M. (1998). The antipsoratic agent dimethylfumarate immunomodulates T-cell cytokine secretion and inhibits cytokines of the psoriatic cytokine network. *British Journal of Dermatology, 139*(390 – 395)

Pena, J.A. and Versalovic, J. (2003). *Lactobacillus rhamnosus* GG decreases TNF-α production in lipopolysaccharide-activated murine macrophages by a content-independent mechanism. *Cellular Microbiology, 5:4*(277 – 285)

Raabe, T., Bukrinsky, M., & Currie, R.A. (1998). Relative contribution of transcription and translation to the induction of tumor necrosis factor-α by lipopolysaccharide. *J. Biol. Chem. 273*(974 – 980)

Ropper, A.H. (2012). The "poison chair" treatment for multiple sclerosis. *N ENGL J MED 367:12*(1149 – 1150)

Scannevin, R.H., Chollate, S., Jung, M., Shackett, M., Patel, H., Bista, P. Zeng, W., Ryan, S., Yamamoto, M., Lukashev, M., & Rhodes, K.J. (2012). Fumarates promote cytoprotection of central nervous system cells against oxidative stress via the nuclear factor (erythroid-derived 2)-like 2 pathway. *The Journal of Pharmacology and Experimental Therapeutics, 341*(274 – 284)

Schimrigk, S., Brune, N., Hellwig, K., Lukas, C., Bellenberg, B., Rieks, M., Hoffman, V., Pohlau, D. & Przuntek, H. (2006). Oral fumaric acid esters for the treatment of active multiple sclerosis: an open-label, baseline-controlled pilot study. *European Journal of Neurology, 13*(604 – 610)

Schmidt, M.M., and Drigen, R. (2010). Fumaric acid diesters deprive cultured primary astrocytes rapidly of glutathione. *Neurochemistry International, 57*(460 – 467)

Taylor, M.F., Paulauskis, J.D., Weller, D.D. & Kobzik, L. (1996). *In vitro* efficacy of morpholino-modified antisense oligomers directed against tumor necrosis factor-α mRNA. *J. Biol. Chem. 271*(17445 – 17452)

Treumer, F., Zhu, K., Glaser, R., & Mrowietz, U. (2003). Dimethylfumarate is a potent inducer of apoptosis in human T cells. *The Journal of Investigative Dermatology, 121:6*(1383 – 1388)

Tsao, L.T., Lin, C.N. & Wang, J.P. (2004). Justicidin A inhibits the transport of tumor necrosis factor-α to cell surface in lipopolysaccharide-stimulated RAW 264.7 macrophages. *Mol. Pharmacol., 65*(1063 – 1069)

Tschopp, J. (2011). Mitochondria: Sovereign of inflammation? *Eur. J. Immunol. 41*(1196 – 1202)

Tweedie, D., Luo, W., Short, R.G., Brossi, A., Holloway, H.W., Li, Y., Yu, Q., Greig, N.H. (2009). A cellular model of inflammation for identifying TNF-α synthesis inhibitors. *J. Neurosci methods, 183:2*(182 – 187)

Virca, G.D., Kim, S.Y., Glaser, K.B., & Ulevitch, R.J. (1989). Lipopolysaccharide induces hyporesponsiveness to its own action in RAW 264.7 cells. *Journal of Biological Chemistry, 264:36*(21951 – 21956)

Wilms, H., Sievers, J., Rickert, U., Rostami-Yazdi, M., Mrowietz, U., & Lucius, R. (2010). Dimethylfumarate inhibits microglial and astrocytic inflammation by suppressing the synthesis of nitric oxide, IL-1β, TNF-α and IL-6 in an in-vitro model of brain inflammation. *Journal of Neuroinflammation, 7:30* (1 – 8)

Yazdi, M.R. and Mrowietz, U. (2008). Fumaric acid esters. *Clinics in Dermatology, 26*(522 – 526)

Yuan, H., Perry, C.N., Huang, C., Iwai-Kanai, E., Carreira, R.S., Glembotski, C.C., Gottlieb, R.A. (2009). LPS-induced autophagy is mediated by oxidative signaling in cardiomyocytes and is associated with cryoprotection. *Am J Physiol Heart Circ Physiol 296*(H470 – H479)